LOSS COEFFICIENT IN A CHANNEL BEND WITH NATURALLY DEFORMED BED. (A-011-PR)

BY

Dr. Christos Hadjitheodorou

WATER RESOURCES RESEARCH INSTITUTE

SCHOOL OF ENGINEERING

MAYAGUEZ, PUERTO RICO

June, 1969

TABLE OF CONTENTS

I. INTRODUCTION

The problem of determining losses of available energy in meandering streams has attracted considerable attention in the recent past. As a result, a number of investigations have been undertaken aiming at a clearer understanding of the effects of various hydraulic parameters on the flow through channel bends. Such investigations include those by Mockmoore (1), Shukry (2), Rozovkii (3), Hayat (4), Yen B.C. (5), and Yen C.L. (6).

Because of the complexity of the problem, most of the above studies have dealt with channels of fixed cross-section and immovable beds. However, it was pointed out in C. L. Yen's (6) investigation, in which he considered the effects of a movable channel bed, that computations of energy losses in meandering rivers based on information obtained in fixed bed studies lead to an underestimate of these losses.

The energy losses in a channel bend with fixed bed are primarily due to an asymmetrical water surface elevation causing asymmetries in the pressure distribution. In the case of a movable bed, which applies to meandering streams, it has been observed that a point bar is commonly formed along the inside of the bed. This bar increases the losses considerably since it acts as an obstacle to the flow, with its accompanying backwater effects.

Considering the fact that adequate information exists concerning the losses

due to the bend itself, it has been the aim of the present investigation to study the effects of a point bar on the flow and to obtain quantitative information with regard to the additional energy losses due to the point bar.

The study consists of two phases; the experimental, in which the flow over an obstacle in a flume was studied in the laboratory, and the analytical in which a theoretical solution is obtained to the same problem.

II. EXPERIMENTAL INVESTIGATION

1. Physical Analysis

It is obvious that flow past a barrier or an obstacle can only take place at the expense of available energy. Consequently, the existence of a point bar in an alluvial stream will cause a reduction of the energy available in the flow. Qualitative discussions of the phenomenon can be found in various texts on hydraulics. Bachmeteff (7) and Chow (8), for example, describe how, due to the energy losses caused by an obstacle in the flow, in the supercritical regime the water surface elevation rises over the obstacle while in subcritical flow the surface elevation drops.

The mechanism of the phenomenon can be understood by considering the flow past the part of the obstacle, or point bar, which rises in the direction of low. Because of the existence of the obstacle, the channel bed rises in the direction of flow and, as a result, the water depth decreases. Consequently, the pressure at a

cross section immediately upstream from the obstacle, is greater than the pressure at the top of the obstacle. One part of this differential pressure force is used to accelerate the flow, while the remaining part is in equilibrium with the boundary reaction due to the obstacle. The tangential component of this reaction increases in the direction of flow on the rising part of the obstacle, while it decreases on the falling part as the flow decelerates. The direction of the tangential component of the reaction is everywhere opposite to the flow direction. The flow, therefore, must do work equal to the tangential component times the flow velocity, thus losing part of the available flow energy.

The tangential component of the reaction due to the obstacle, or point bar, increases the channel bed shear stress to a magnitude which is greater than the shear stress applicable to uniform flow over an equivalent length of level bed. Additional energy is dissipated as the tangential component of the reaction is transmitted into the flow by means of viscous and/or turbulent friction. The drop of water surface elevation across the obstacle, in addition to that of uniform flow, represents the additional loss of energy in this case. In case the flow separates from the boundary, an even greater amount of energy is dissipated because of increased asymmetries in pressure distribution along the obstacle and the formation of eddies. Finally, waves formed on the water surface because of the existence of the obstacle reduce the available flow energy by means of wave drag.

a. Frictional effects

The amount of energy dissipated through boundary friction is directly proportional to the friction factor, f. In general, the friction factor is a function of the Reynolds Number, Re, the relative roughness, and the properties of the flow cross-sectional area. In laminar flow, where viscous forces are predominant, it varies inversely with Re. In turbulent flow, in the case of smootle boundaries, f decreases with Re-Chow (8), Reinus (9).

In this investigation, all flows were well within the turbulent regime. Furthermore, for each obstacle the geometric properties of the flow area were kept constant, while the channel and obstacle surfaces were hydraulically smooth.

b. Separation

Rapid changes in boundary allignment, in general, cause local pressure gradients in excess of the pressure gradient of the main flow. If the pressure gradient is positive in the direction of flow, the pressure forces in combination with the shear forces tend to reduce the momentum of the flow. However, since the momentum is already zero at the boundary, further reduction of the momentum is physically impossible and a flow discontinuity results at the boundary. In other words, the flow can continue downstream only by separating from the boundary.

Increased velocities and low pressures occur throughout the zone of separation. The assymetric pressure distribution causes a net force known as form drag. Energy from the mean flow is lost equivalent to the amount of work done in counteracting the form drag.

c. Wave drag

Open channel flow past an obstacle is classified as non-uniform. The presence of the obstacle causes waves to form on the water surface. The characteristics of these waves depend on the Froude Number, Fr, and the flow geometry. In the subcritical regime, which is the one examined in this study, the waves extend upstream resulting in changes in the depth of flow. The variations in water-surface elevation cause assymmetric pressure distributions across the obstacle which, in turn, result in drag.

The part of the drag which generates and maintains the surface waves is the wave drag. As the Froude Number increases the wave drag is expected to increase. The reason for this is that with increasing Fr, the wave celerity approaches the magnitude of the flow velocity. As a result, the wave will extend a shorter distance upstream as Fr increases. Consequently, the asymmetry in surface elevation and pressure increases with Fr, which leads to greater values for the wave drag.

2. Dimensional Analysis

The most important parameters involved in open channel flow past an obstacle are the following:

H_L = energy per unit weight of fluid (head) lost due to the obstacle,

V = mean flow velocity,

h = mean depth of flow,

d = obstacle height,

ν = kinematic viscosity of water, and

g = acceleration due to gravity.

Applying the principles of dimensional analysis to the above variables one may write

$$f(H_L, V, h, d, \nu, g) = 0$$

The fundamental dimensions in f are length and time. Hence four dimensionless π groups may be formed by the six variables in f, which may then be written as:

$$g_1\left(\frac{H_L}{V^2/2g}, \frac{h}{d}, \frac{V}{\sqrt{gh}}, \frac{Vh}{\nu}\right) = 0$$

Using the definitions

$$C_L = \frac{H_L}{V^2/2g} = \text{loss coefficient},$$

$$F_r = \frac{V}{\sqrt{gh}} = \text{Froude Number, and}$$

$$Re = \frac{Vh}{\nu} = \text{Reynolds Number}$$

the function g_1 can be transformed

$$C_L = F\ (Re, Fr, \frac{h}{d})$$

The Reynolds Number affects C_L through its influence on separation and surface friction. Experiments were conducted with obstacles of various shapes until no separation could be detected by either inspection or by means of dyes introduced

in the flow. Furthermore, the loss due to friction for an equivalent length of channel was subtracted from the total loss of head. In that way the influence of Re on C_L is expected to have been minimal. Thus the objective of the experimental investigation has been to determine the dependence of the loss coefficient, C_L, on the Froude Number, Fr, and on the relative depth h/d, for obstacles over which no separation effects were present.

3. Equipment and Procedure

a. Equipment

Experiments were conducted in a rectangular, tilting flume located in the Laboratory of Fluid Mechanics of the University of Puerto Rico at Mayaguez. The flume has a width of 18 inches and is 25 feet long. As shown in figure 1, the walls of the flume are made of glass while the bottom is steel which has been painted to avoid corrosion and to minimize the frictional retardation of the flow. A tail gate at the flume exit serves to control the flow. Water is circulated by means of a pump, which drives the water into a supply tank located at the upstream end of the flume. The supply tank serves as an aid to the uniformity of flow. The amount of flow can be varied by means of a valve at the discharge end of the pump. Flowrates are measured in a volumetric tank located at the flume exit as shown in figure 2.

A number of piezometer holes were drilled at the bottom of the flume and were connected by means of plastic tubes to an air-water manometer shown in figure 3.

The manometer was used to measure depth of flow as described below. The point gages shown in figure 1 were also used in the determination of depth.

The obstacles were made of wood with surfaces cut as smooth as possible and painted. The shape of the obstacles was approximately sinusoidal. In the initial stages of the investigation, plaster of paris was used to modify the obstacle shape until separation effects were avoided.

Note: The meandering channel described in the proposal was never constructed because of lack of space and the required technical personnel for such construction.

b. Measurement of depth

An arbitrary datum plane was established by placing the flume in the horizontal position, raising the tail gate and filling the flume with water to a certain depth. The water surface and flume bottom elevations at all piezometer holes were measured by means of point gages. The point on the channel bed directly above the flume pivot was selected as datum, and the water depth at that point was also measured. The difference between the depth at datum and that at each piezometer hole gave the bed profile with reference to the datum. The distance of the datum point from each of the piezometer holes was measured and used to compute changes in elevation due to tilting of the flume.

c. Determination of head loss

Since the width of the flume remained constant, the flow cross-sectional area

could be computed by multiplying the width times the depth obtained from the manometer readings. The mean velocity, V, could then be obtained by dividing the flowrate by the cross-sectional area at each section. The total head at each section was obtained by adding the velocity head, the depth and the elevation. Loss of head due to the obstacle was computed as the difference of total head values up-stream and downstream of the obstacle, with a appropriate adjustment for frictional effects.

4. Results and Conclusions

The experimental data were collected with the two previously stated objectives in mind, namely, to obtain the form in which variations in the Froude Number, Fr, and variations in the relative depth, h/d, affect the loss coefficient, C_L. The data were compiled and analyzed using the hiah speed digital computer, located on the Mayaguez Campus of the University of Puerto Rico. The results are shown on figures 4 and 5.

Figure 4 is a plot of Froude Number versus loss coefficient. According to the preceding discussion, the water surface profile varies with the Froude Number resulting in an asymmetric pressure distribution along the obstacle. This asymmetry in the pressure distribution gives rise to a net longitudinal force on the boundary. The loss of available energy is due to the work done by the fluid in moving against the equal and opposite force applied on it by the obstacle.

At low values of the Froude Number, the asymmetry in the water surface

elevation and the consequent asymmetry in the pressure is very small. Hence, the effect of Fr on the loss coefficient is negligible. This is clearly shown on figure 4 in which the loss coefficient has very nearly constant values for Fr varying from 0.15 to 0.45. In this range of Fr, since variations in wave drag are negligible, any variations in the longitudinal drag could be attributed to frictional effects. However, no such effect is evident from the results for the experimental range of Re from 10^4 to 10^5. Finally, figure 4 indicates that for Froude Numbers up to 0.45, C_L is independent of Fr and depends primarily on relative depth h/d.

With increasing values of the Froude Number the entire wave on the water surface, created by the obstacle, shifts downstram. The shifting creates greater asymmetries in pressure distributions along the obstacle leading to an increase in the net longitudinal force on the boundary. The flow spends greater amounts of energy in overcoming the boundary reaction, a fact made obvious by the increasing valves of C_L for Fr from 0.45 to 0.70 on figure 4. Nevertheless, in this Fr range also, the effect of relative depth on C_L is very pronounced.

Figure 5 shows the variation of the loss coefficient with relative depth for Froude Numbers in a close neighborhood of 0.4. As h/d increases C_L decreases, since the effects of the obstacle on the flow diminish with an increase of depth of water over the obstacle. However, the rate of decrease of C_L for h/d up to about 5 is much greater than that for C_L for h/d greater than 5.

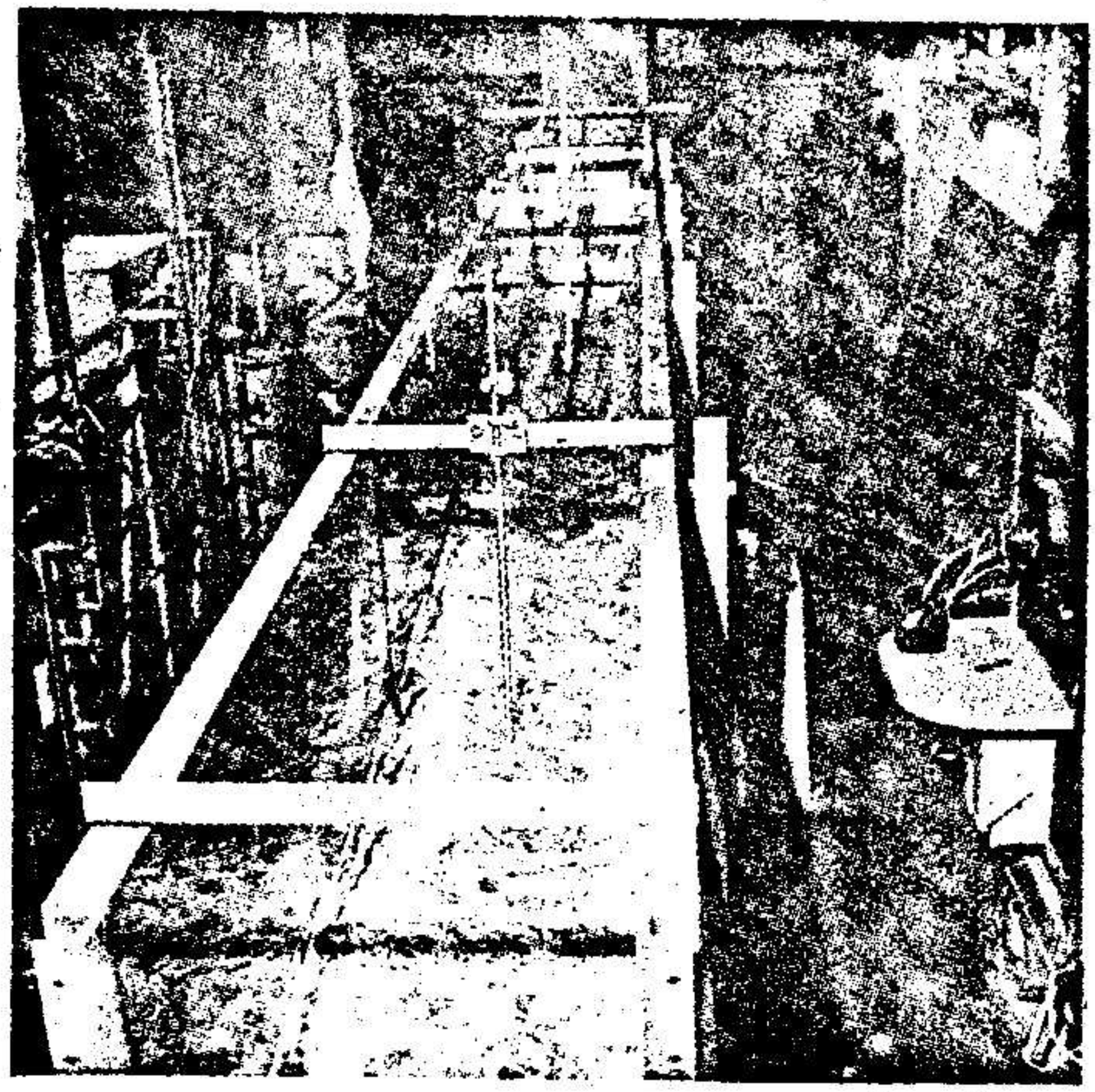

Fig. 1 The rectangular flume

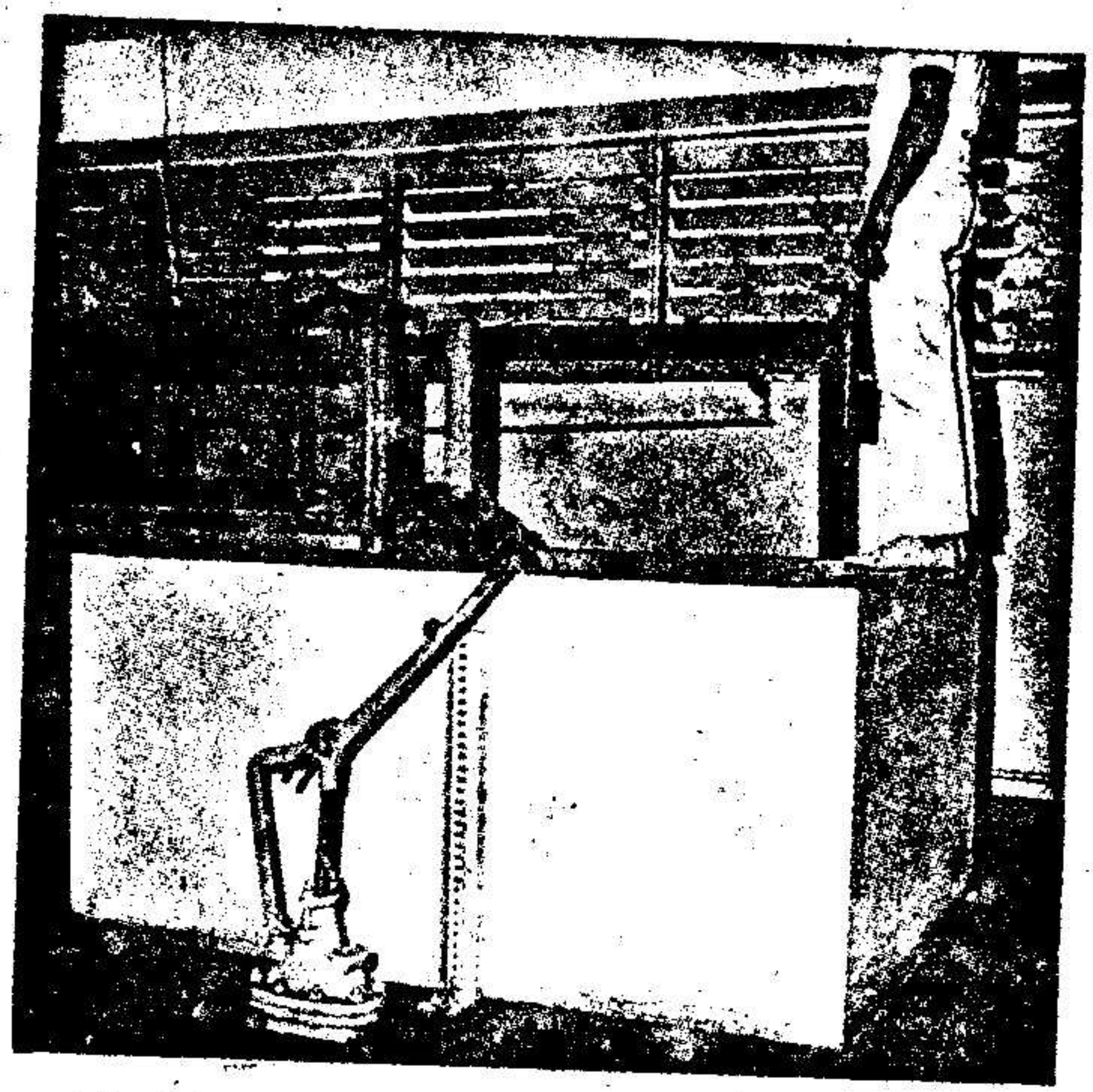

Fig. 2. Volumetric tank

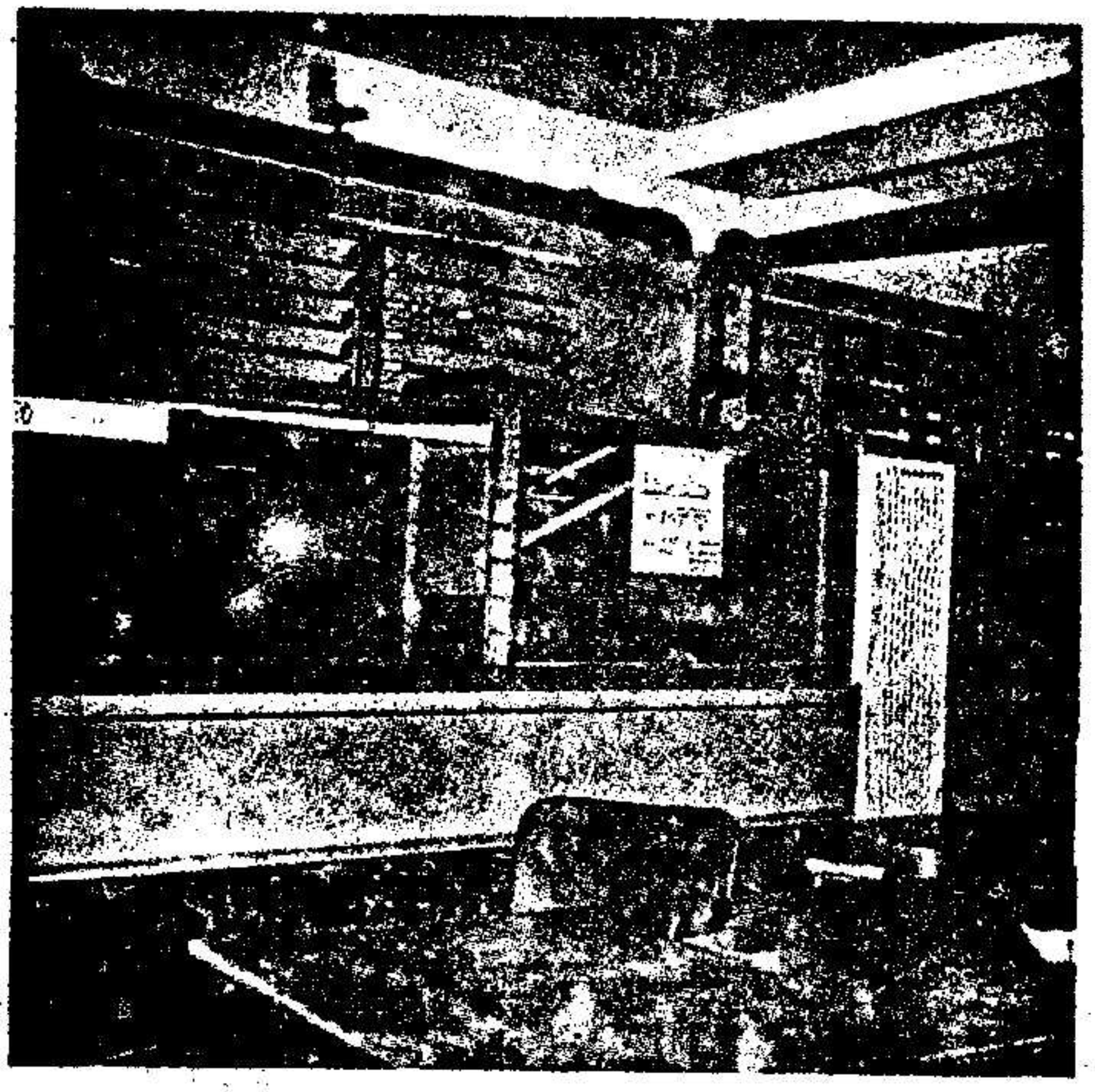

Fig. 3. Air-water manometer

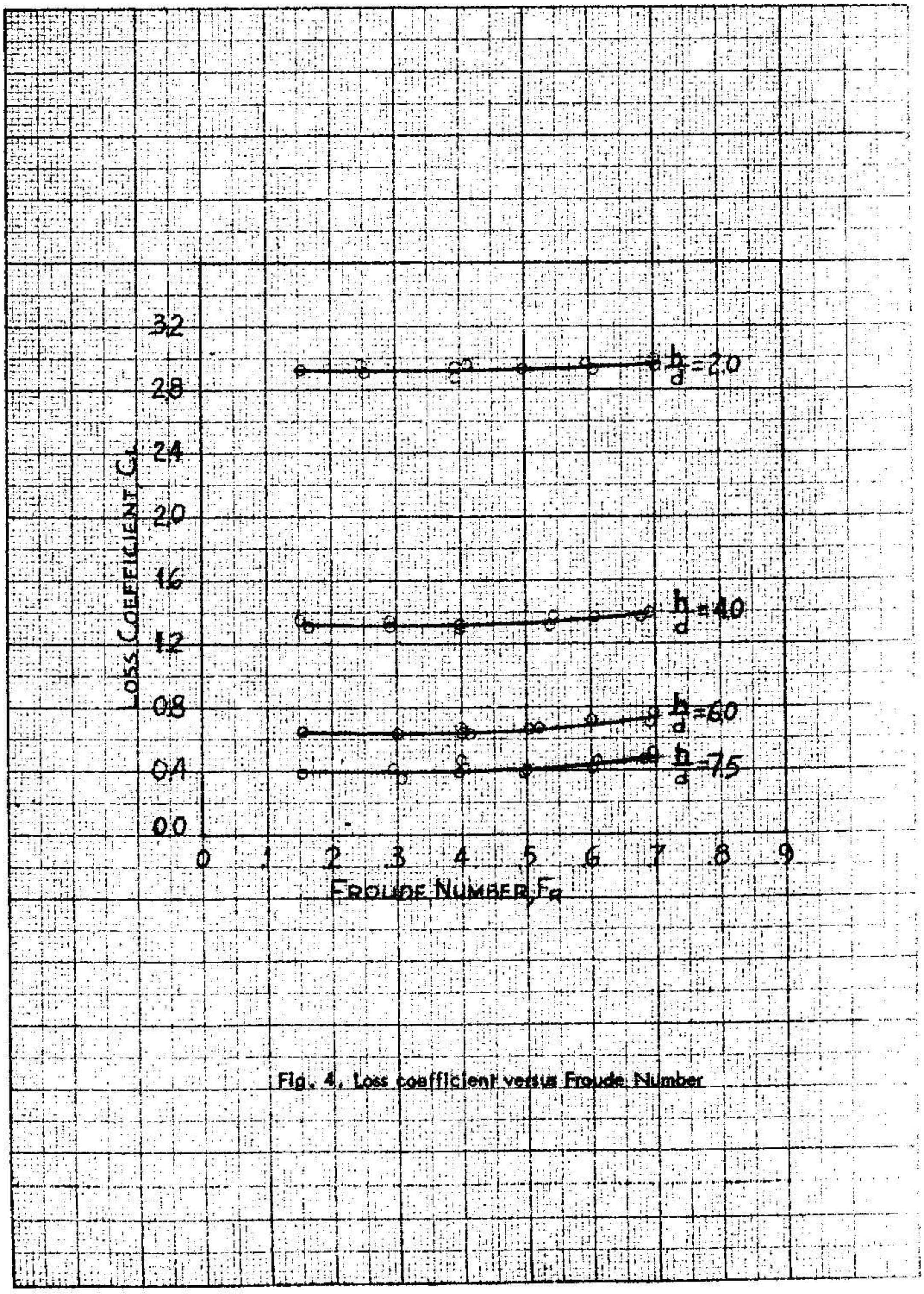

Fig. 4. Loss coefficient versus Froude Number

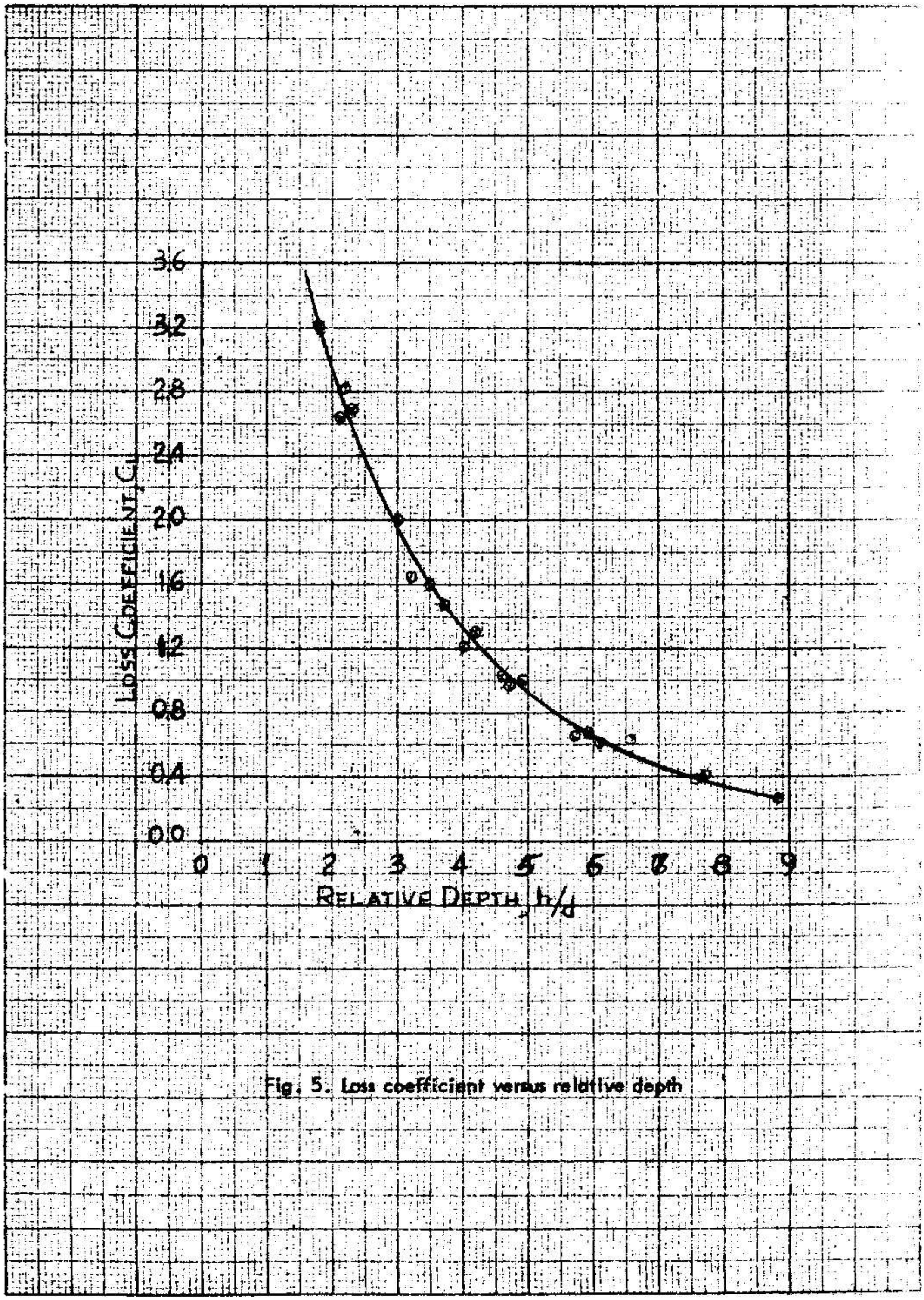

Fig. 5. Loss coefficient versus relative depth

III. ANALYTICAL SOLUTION

1. The Problem

Losses of energy in open channel flow over an obstacle could easily be computed if, given information concerning the geometry of the obstacle as well as flow data such as flow rate or depth upstream, an analytical solution could be developed to yield flow velocities and the water surface profile over the obstacle. Such a solution to the problem is presented here, developed according to the theory of flow of ideal jets in which gravity is a predominant force and surface waves are excluded. A complete discussion of the theory can be found in Gurevich (10). A similar problem, that of flow over a spillway, was solved by Duisheev (11), however his solution, as will subsequently pointed out, cannot very well be applied to a practical problem.

The flow field in the complex plane $z = x+iy$ is as shown in figure 6. The problem is essentially solved once the complex potential

$$w(z) = \varphi(z) + i\,\psi(z) \tag{1}$$

is determined, where φ and ψ are the velocity potential and the stream function respectively. The boundary conditions on the flow require that the normal component of the velocity vanish on all solid boundaries, i.e.

$$\psi = \text{constant, or } \frac{\partial \varphi}{\partial n} = 0 \text{ on solid boundaries} \tag{2}$$

and that the pressure be constant on the free surface, or according to Bernoulli

$$\frac{v^2}{2} + gy = \text{constant on free surface} \tag{3}$$

The main difficulty in the problem arises from the fact that the position of the free

surface is not known a priori.

Following the procedure first used by Zhukovskii (12) an additional complex variable is defined as

$$\omega = \ln \frac{dw}{dz} \tag{4}$$

The solution then involves mapping the functions ω and w onto the upper-half plane of the parametric variable $t = \xi + i\eta$. Once w(t) and $\omega(t)$ are determined

$$z(t) = \int \exp[-w(t)] \frac{dW(t)}{dt} dt \tag{5}$$

2. Determination of w(t) and $\omega(t)$

a Mapping of w(t).

According to (2), the stream function should be constant on all solid boundaries Letting $\psi = 0$ on the channel bed FABCDE, from the theorem in elementary fluid mechanics it follows that $\psi = q$ on the free surface, where q is the flowrate. The region of change of w, therefore, is an infinite strip of width q, as shown on figure 7a.

The strip in figure 7a can be considered as a polygon with infinitely extended vertices at F and E and angles equal to zero at these points. The Schewarz - Christofell transformation maps the polygon into the real axis of t according to

$$w = \frac{q}{\pi} \ln \frac{t-1}{t+1} \tag{6}$$

As shown in figure 7b, where the lower case letters correspond to the capitals in 7a, the unknown free surface maps into the straight line from $t = -1$ to $= 1$.

b. Determining $\omega(t)$

Following Duisheev (11) an auxiliary function is introduced

$$F(t)=\frac{\omega(t)}{\sqrt{t^2-1}}=\frac{\ell n(dw/dz)}{\sqrt{t^2-1}}=\frac{\ell nv-i\vartheta}{\sqrt{t^2-1}} \qquad (7)$$

where v is the velocity vector and ϑ is the angle between the direction of v and the positive xaxis. Obviously, once $F(t)$ is determined, $\omega(t)$ is known also. $F(t)$ can be found on the upper half-plane of t once the imaginary part, $\mathrm{Im}F(t)$, is determined, according to the equation

$$F(t)=\frac{1}{\pi}\int_{-\infty}^{\infty}\frac{\mathrm{Im}F(\xi)}{\xi-t}\,d\xi \qquad (8)$$

The channel bottom is a streamline, therefore, $\vartheta(t)$ is known all along FABCDE. $\mathrm{Im}F(t)$ can be determined on the solid boundaries as follows;

On O'BAF

$$\mathrm{Im}F(t)=\frac{-\vartheta(t)}{\sqrt{t^2-1}} \qquad (t\geq 1) \qquad (9a)$$

On O'CDE

$$\mathrm{Im}F(t)=\frac{\vartheta(t)}{\sqrt{t^2-1}} \qquad (t\leq -1) \qquad (9b)$$

On the free surface EOF

$$\mathrm{Im}F(t)=\frac{-\ell nv}{\sqrt{1-t^2}} \qquad (-1<t<1) \qquad (9c)$$

Substituting equations (9) into (8) and using the known values of $\vartheta(t)$ -see figure 6- yields

$$F(t)=-\frac{\alpha}{\pi}\int_{-c}^{-d}\frac{d\xi}{(\xi-t)\sqrt{\xi^2-1}}-\frac{1}{\pi}\int_{-1}^{1}\frac{\ell nv\,d\xi}{(\xi-t)\sqrt{1-\xi^2}}-\frac{\beta}{\pi}\int_{a}^{b}\frac{d\xi}{(\xi-t)\sqrt{\xi^2-1}} \qquad (10)$$

The second integral on the right hand side of (10) cannot be evaluated because

the velocity, v, is not known. This difficulty can be by-passed by assuming a form v, on the free surface, such that

$$\ln v(\xi) = \sum_{k=0}^{n} a_k (\xi - 1)^k \qquad (11)$$

where the a_k are unknown real coefficients to be determined from the boundary conditions on the free surface, while

$$\ln v\ (1) = \ln v_F = a_o$$

In addition to the coefficients in (11), the parameters a,b,c, and d need also be determined. One of the four parameters can be assigned arbitrarily because in the Schwarz-Christoffel transformation only two of the allowable three arbitrary parameters were given values ($t_F = 1$, $t_E = -1$). The remaining three parameters - for example a,b,c - can be computed from the known obstacle dimensions AB, BC, and CD. Duisheev (11) solves the problem in an inverse fashion. He arbitrarily defines a,b, and c and then computes the spillway dimensions AB, BC, CD. The solution is greatly simplified in this manner, however its practical applicability is not altogether obvious.

3. Computation of a_k, a, b, and c.

The accuracy of the solution increases as the number n of the coefficients in (11) increases. Nevertheless, a good approximation is obtained if the series (11) is limited to the first two terms with

$$a_2 = a_3 = \ldots = a_n = 0$$

In this case, using the boundary condition (3) in the transformed form

$$\frac{t^2-1}{2P/\rho} v^2 \frac{dv}{dt} = -g \sin\vartheta \tag{12}$$

where p is pressure and ρ is fluid density, together with the continuity equation,

$$h_F v_F = h_E v_E = q \tag{13}$$

the following equation for a_1 results after a fair amount of algebraic manipulation

$$a_1 = -\frac{C_1}{C_2} \pm \left[\left(\frac{C_1}{C_2}\right)^2 - \frac{C_3}{C_2} \right]^{1/2} \tag{14}$$

Where

$$C_1 = -\pi + \sin\alpha \cdot M_1(t) - \sin\beta \cdot N_1(t) + 2(\sin\vartheta_1 + \cos\vartheta_1)$$

$$C_2 = -2(\pi+1) + \sin\alpha \cdot M_2(t) - \sin\beta \cdot N_2(t) + 4.7\sin\vartheta_1 + 4\cos\vartheta_1$$

$$C_3 = 2\sin\alpha \cdot M_0(t) - 2\sin\beta \cdot N_0(t) + 4\sin\vartheta_1$$

and

$$\vartheta_1 = -\frac{\alpha}{\pi}\left(\operatorname{arctn}\sqrt{c^2-1} - \operatorname{arctn}\sqrt{d^2-1}\right) - \beta/\pi\left(\operatorname{arctn}\sqrt{a^2-1} - \operatorname{arctn}\sqrt{b^2-1}\right)$$

$$M_K(t) = \int_{-c}^{-d} C_4 \cdot C_5 \cdot \frac{\left[1-\left(t+\sqrt{t^2-1}\right)\right]^K}{t^2-1}\,dt$$

$$N_K(t) = \int_{a}^{b} C_6 \cdot C_7 \cdot \frac{\left[1-\left(t-\sqrt{t^2-1}\right)\right]^K}{t^2-1}\,dt$$

The coefficients C_4 through C_7, which are functions of a,b,c,d, and t are given in the Appendix.

The coefficient a_1 can be computed from (14) given the parameters a,b,c, and

d. Having arbitrarily defined d, the ramaining three parameters can be found with the aid of the following expressions for the known obstacle dimensions AB, BC, and CD;

$$AB = 2\frac{q}{\pi}\exp(-\alpha_o)\cdot N(t) \tag{15}$$

$$CD = 2\frac{q}{\pi}\exp(-\alpha_o)\cdot M(t) \tag{16}$$

Where

$$N(t) = \int_{a}^{b} C_6 \cdot C_7 \cdot \frac{\exp[\alpha_1 - \alpha_1(t-\sqrt{t^2-1})]}{t^2-1}\,dt \tag{16a}$$

and

$$M(t) = \int_{-c}^{-d} C_4 \cdot C_5 \frac{\exp[\alpha_1 - \alpha_1(t+\sqrt{t^2-1})]}{t^2-1}\,dt \tag{16b}$$

$$BC = -2\frac{q}{\pi}\exp(-\alpha_o)\cdot[P(\tau)+R(\tau)] \tag{17}$$

where, defining a new variable $\tau = 1/t$,

$$P(\tau) = \int_{0}^{-1/c} C_8 \cdot C_9 \cdot \frac{\exp\left[\alpha_1 - \alpha_1\left(\frac{1}{\tau}+\sqrt{\frac{1}{\tau^2}-1}\right)\right]}{1-\tau^2}\,d\tau$$

$$R(\tau) = \int_{1/b}^{0} C_{10} \cdot C_{11} \frac{\exp\left[\alpha_1 - \alpha_1\left(\frac{1}{\tau}-\sqrt{\frac{1}{\tau^2}-1}\right)\right]}{1-\tau^2}\,d\tau$$

Similarly, because of their complexity, the coefficients C_8 through C_{11}, all functions of a, b, c, d and τ are given in the Appendix.

It should be noted that equations (15), (16), and (17) all involve the term $q\cdot\exp(-\alpha_o)$. It can easily be shown, however, that

$$h_F = q \cdot \exp(-a_o).$$

Thus, given the undisturbed depth, h_F, upstream of the obstacle, as well as the obstacle dimensions, equations (14) through (17) form a system which can be solved simoultaneously to yield α_1, a, b, and c.

4. Computer Solution

The system of simultaneous equations (14) through (17) because of its complexity can only be solved by means of a digital computer. The solution involves an iteration process according to which initial values of a,b,and c are chosen, a_1 and the integrals in (15), (16), (17) are computed numerically and the results are compared to the given values of AB, BC, CD. New values, as required, of a,b,c are computed and the process is repeated until the difference between given and computed values is negligible.

The iteration process used is an extension of the "Newton-Raphson algorithm" as described by Lapidus (13). Given a system of equations

$$f_i(s_1, s_2, \cdots, s_n) = 0 \quad ; \quad i = 1, 2, \ldots, n \qquad (18)$$

it is desired to find the values of $\bar{s}_i$ such that substitution into the system of equations will satisfy (18) identically. Letting s_r denote the initial values of the variables s_i, and defining $\bar{s}_r - s_r = \Delta s_r$, the initial values s_r can be adjusted by solving the following system for Δs_r

$$\sum_{r=1}^{n} \frac{\partial f_i}{\partial s_r} \Delta s_r - f_i(s_1, s_2, \cdots, s_n) = 0$$

Once s_r are computed the iteration continues for new values $s_r' = s_r + \Delta s_r$.

The integrals were evaluated using the rectangular formula because it does not involve evaluation of the integrand at the limits of integration. It can be verified by inspection that the integrands in equations (14) through (17) pocess singularities at some of the limits. In case it is desired to use either the trapezoidal formula or Simpson's rule for computing the integrals, the integrands can be rid of the singularities by a simple application of a Taylor's expansion about each singularity. However, this process makes the integrands even more complicated then they already are.

5. The Free Surface

All points on the free surface of the fluid are mapped on the real axis of plane t in the segment $-1 < t < 1$. Considering any such point G on the free surface, which maps in the t-plane a distance r from F ($t = 1$), there is a related point H lying on the channel bottom segment FA, which maps on the t-plane such that

$$FG = r = FH \qquad \text{(on t-plane)}$$

The coordinates of H in the z-plane (the flow plane) can easily be found as

$$\begin{aligned} y_H &= 0 \\ x_H &= 2\frac{q}{\pi} \exp(-\alpha_o) \cdot N'(t) \end{aligned} \tag{19}$$

where $N'(t)$ is the integral from a to $(1 + r)$ of the integrand in $N(t)$ given by equation (16a).

The coordinates of point G lying on the free surface in the flow plane z can be computed from

$$x_G - x_H = 2\frac{q}{\pi}\exp(-\alpha_0)\cdot\int_0^{\pi} R(\sigma)\,d\sigma \qquad (20a)$$

$$y_G - y_H = 2\frac{q}{\pi}\exp(-\alpha_0)\int_0^{\pi} S(\sigma)\,d\sigma \qquad (20b)$$

Where the new variable σ is defined by

$$t = 1 + r\exp(i\sigma)\ ;\ 0 \le \sigma \le \pi \qquad (21)$$

It is obvious that when $\sigma = 0$, $t = 1+r$, i.e. the position of point H on the t-plane, while when $\sigma = \pi$, $t = 1-r$ i.e. point G on the t-plane.

Furthermore

$$R(\sigma) = \frac{D_1}{D_2}\cdot\left[\cos\alpha_1\cdot\sin\sigma - (2+r\cos\sigma)\cdot\sin\alpha_1\right]$$

$$S(\sigma) = \frac{D_1}{D_2}\left[(2+r\cos\sigma)\cdot\cos\alpha_1 + r\cdot\sin\sigma\cdot\sin\alpha_1\right]$$

$$\alpha_1 = \left[\frac{\alpha}{\pi}\gamma + \beta\gamma_1 - \alpha_1(r\sin\sigma - \sqrt{r_1}\cdot\sin\frac{\beta'}{2})\right]$$

with $D_1, D_2, \alpha_1, \beta', \gamma$, and γ_1 given in the Appendix.

It is now possible to compute the coordinates (x,y) for any point on the free surface by the following equations in parametric form. For points between G and F ($t = 1$)

$$x_G - x_H = -2\frac{q}{\pi}\exp(-\alpha_0)\cdot N_1(t,\vartheta) \qquad (21a)$$

$$y_G - y_H = +2\frac{q}{\pi}\exp(-\alpha_0)\cdot N_2(t,\vartheta) \qquad 21b)$$

and for points between G and E ($t = -1$)

$$x_G - x_H = -2\frac{q}{\pi}\exp(-\alpha_0)\cdot N_1(t,\vartheta) \qquad (22a)$$

$$y_G - y_H = -2\frac{q}{\pi}\exp(-\alpha_0)\cdot N_2(t,\vartheta) \qquad (22b)$$

with

$$N_1(t,\vartheta) = \int_{t_G}^{t} \frac{\exp[\alpha_1(1-t)]\cdot\cos\vartheta}{1-t^2}\,dt$$

$$N_2(t,\vartheta) = \int_{t_G}^{t} \frac{\exp[\alpha_1(1-t)]\sin\vartheta}{1-t^2}\,dt$$

Once the position of the free surface is plotted, total head for various points and head loss over the obstacle can be computed as described in paragraph 3c of chapter II. This has been done for an obstacle 1 inch in height and 30°slopes with varying upsteam depths. The results will be included in a paper which is being prepared for publication.

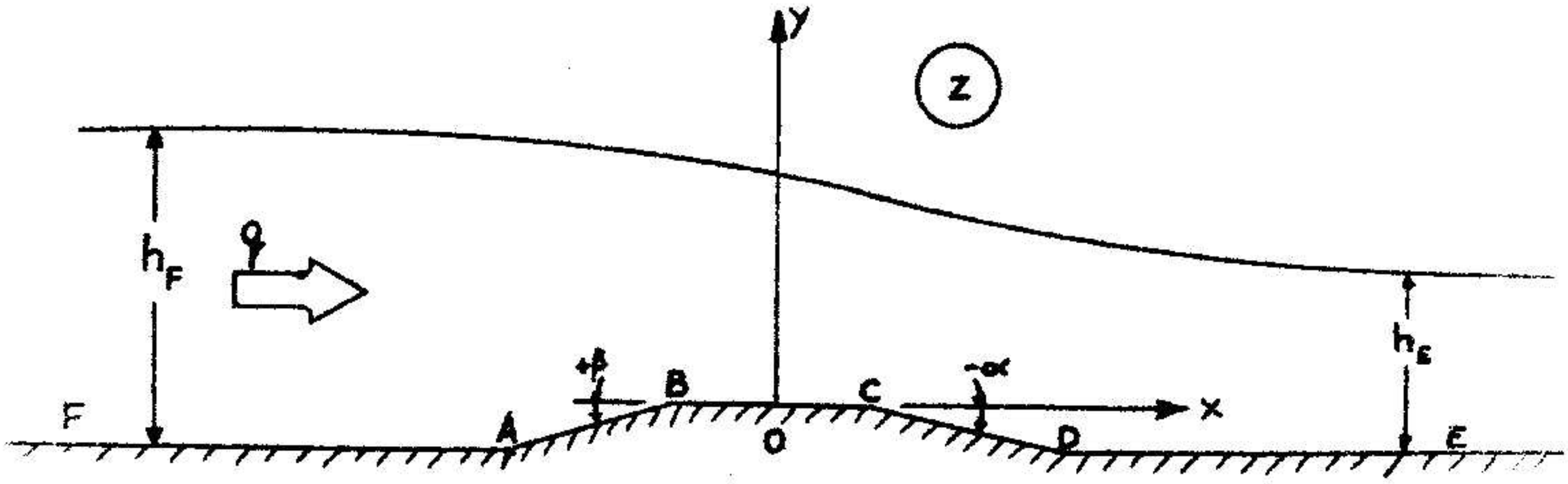

Fig. 6. The flow plane

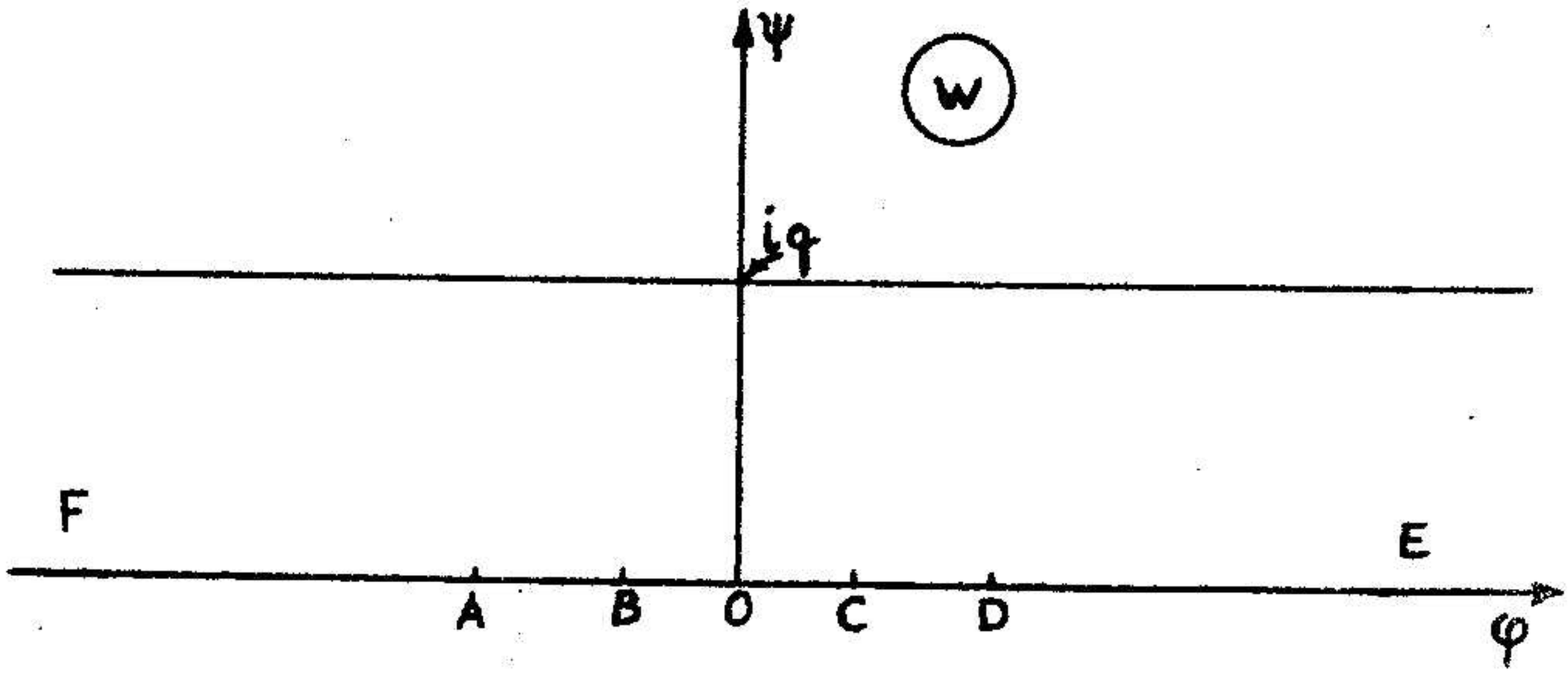

Fig. 7a. The w-plane

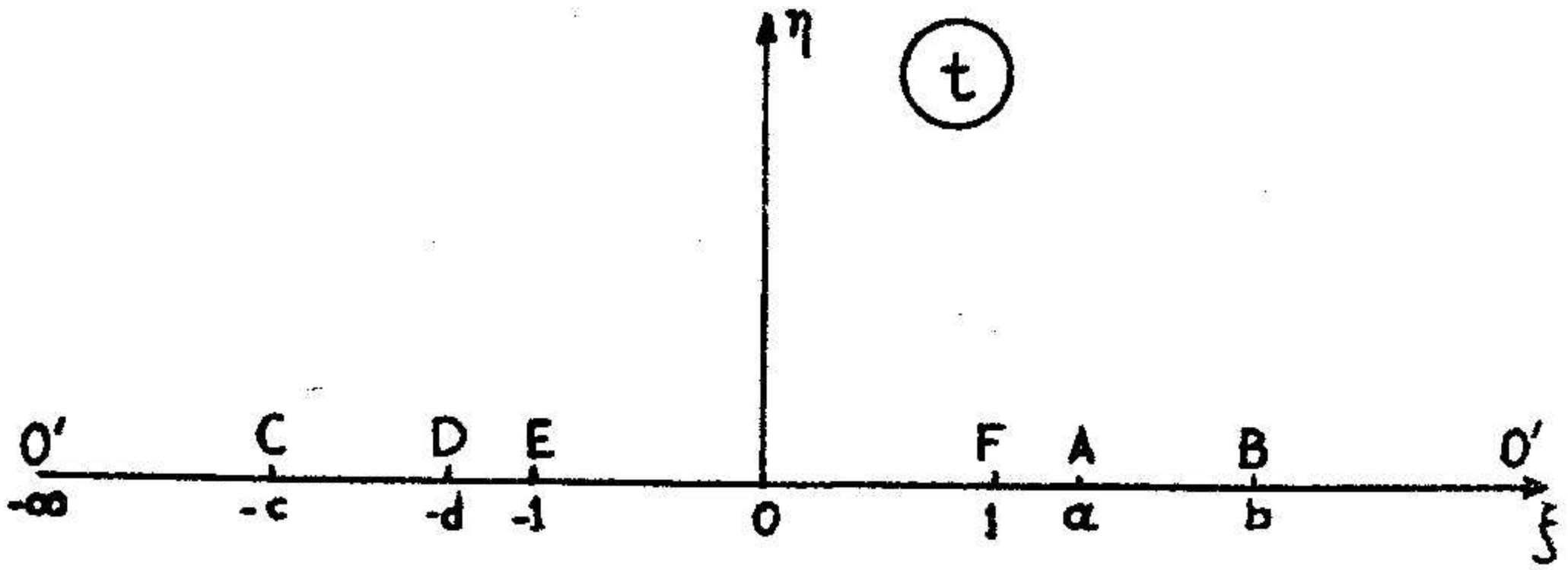

Fig. 7b. The t-plane

APPENDIX

$$C_4=\left\{\frac{(c+t)(td+1-\sqrt{d^2-1}\sqrt{t^2-1})}{(-d-t)(ct+1-\sqrt{c^2-1}\sqrt{t^2-1})}\right\}^{\alpha/\pi}$$

$$C_5=\left\{\frac{(b-t)(at-1-\sqrt{a^2-1}\sqrt{t^2-1})}{(a-t)(tb-1-\sqrt{b^2-1}\sqrt{t^2-1})}\right\}^{\beta/\pi}$$

$$C_6=\left\{\frac{(d+t)(ct+1-\sqrt{c^2-1}\sqrt{t^2-1})}{(c+t)(td+1-\sqrt{d^2-1}\sqrt{t^2-1})}\right\}^{\alpha/\pi}$$

$$C_7=\left\{\frac{(b-t)(at-1+\sqrt{a^2-1}\sqrt{t^2-1})}{(t-a)(bt-1+\sqrt{b^2-1}\sqrt{t^2-1})}\right\}^{\beta/\pi}$$

$$C_8=\left\{\frac{(c\tau+1)(d+\tau-\sqrt{d^2-1}\sqrt{1-\tau^2})}{(d+1)(c+\tau-\sqrt{c^2-1}\sqrt{1-\tau^2})}\right\}^{\alpha/\pi}$$

$$C_9=\left\{\frac{(b\tau-1)(a-\tau-\sqrt{a^2-1}\sqrt{1-\tau^2})}{(a\tau-1)(b-\tau-\sqrt{b^2-1}\sqrt{1-\tau^2})}\right\}^{\beta/\pi}$$

$$C_{10}=\left\{\frac{(\tau d+1)(c+\tau-\sqrt{c^2-1}\sqrt{1-\tau^2})}{(c\tau+1)(d+\tau-\sqrt{d^2-1}\sqrt{1-\tau^2})}\right\}^{\alpha/\pi}$$

$$C_{11}=\left\{\frac{(1-b\tau)(a-\tau+\sqrt{a^2-1}\sqrt{1-\tau^2})}{(1-a\tau)(b-\tau+\sqrt{b^2-1}\sqrt{1-\tau^2})}\right\}^{\beta/\pi}$$

$$D_1 = r_2^{\alpha/\pi} \cdot r_3^{\beta/\pi} \cdot \exp\left[-\alpha_1 \left(r\cos\theta - \sqrt{r_1}\cdot\cos\frac{\beta'}{2}\right)\right]$$

$$D_2 = \left(A_1^2+B_1^2\right)^{\alpha/\pi}\cdot\left(A_2'^2+B_1'^2\right)^{\beta/\pi}\cdot\left(4+r^2+4r\cdot\cos\theta\right)$$

$$r_1 = r\left(4+r^2+4r\cdot\cos\theta\right)^{1/2}\ ;\ r_2 = \left[\left(AA_1+BB_1\right)^2+\left(A_1B-AB_1\right)^2\right]^{1/2}$$

$$r_3 = \left[\left(A_1'A'+B'B_1'\right)^2+\left(A_1'B'-A'B_1'\right)^2\right]^{1/2}\ ;\ \gamma = \operatorname{arctn}\left[\frac{A_1B-AB_1}{AA_1-BB_1}\right]$$

$$\gamma_1 = \operatorname{arctn}\left[\frac{A_1'B'-A'B_1'}{A'A_1'+B'B_1'}\right]\ ;\ \beta' = \operatorname{arctn}\left[\frac{2\sin\theta+r\sin2\theta}{2\cos\theta+r\cos2\theta}\right]$$

$$A = (d+1+r\cos\theta)\cdot(1+c+cr\cdot\cos\theta) - cr^2\cdot\sin^2\theta - \\ -\sqrt{c^2-1}\cdot\sqrt{r_1}\cdot\left[(d+1+r\cdot\cos\theta)\cdot\cos\frac{\beta'}{2} - r\cdot\sin\theta\cdot\sin\frac{\beta'}{2}\right]$$

$$A_1 = (c+1+r\cdot\cos\theta)\cdot(1+d+rd\cdot\cos\theta) - r^2d\cdot\sin^2\theta - \\ -\sqrt{d^2-1}\cdot\sqrt{r_1}\cdot\left[(c+1+r\cos\theta)\cdot\cos\frac{\beta'}{2} - r\cdot\sin\theta\cdot\sin\frac{\beta'}{2}\right]$$

$$A' = (b-1-r\cos\theta)\cdot(\alpha-1+r\cos\theta) + r^2\alpha\cdot\sin^2\theta + \\ +\sqrt{\alpha^2-1}\cdot\sqrt{r_1}\cdot\left[(b-1-r\cos\theta)\cos\frac{\beta'}{2} + r\sin\theta\cdot\sin\frac{\beta'}{2}\right]$$

$$A_1' = (\alpha-1-r\cos\theta)\cdot(b-1+r\cos\theta) + r^2b\cdot\sin^2\theta + \\ +\sqrt{b^2-1}\cdot\sqrt{r_1}\cdot\left[(\alpha-1-r\cos\theta)\cdot\cos\frac{\beta'}{2} + r\sin\theta\cdot\sin\frac{\beta'}{2}\right]$$

$$B = c\cdot(2r\cdot\sin\theta + r^2\sin2\sigma) + (dc+1)\cdot r\sin\theta - \\ -\sqrt{c^2-1}\cdot\sqrt{r_1}\cdot\left[(d+1+r\cos\theta)\cdot\sin\frac{\beta'}{2} + r\sin\theta\cdot\cos\frac{\beta'}{2}\right]$$

$$B_1 = d\cdot(2r\cdot\sin\sigma + r^2\sin 2\sigma) + (dc+1)\cdot r\sin\sigma -$$
$$-\sqrt{d^2-1}\cdot\sqrt{r_1}\cdot\left[(c+1+r\cos\sigma)\cdot\sin\frac{\beta'}{2} + r\sin\sigma\cdot\cos\frac{\beta'}{2}\right]$$

$$B' = (ab+1)\cdot r\sin\sigma - a\cdot(2r\cdot\sin\sigma + r^2\sin^2\sigma) +$$
$$+\sqrt{a^2-1}\cdot\sqrt{r_1}\cdot\left[(b-1+r\cdot\cos\sigma)\cdot\sin\frac{\beta'}{2} + r\sin\sigma\cdot\cos\frac{\beta'}{2}\right]$$

$$B_1' = (ab+1)\cdot r\sin\sigma - b(2r\cdot\sin\sigma + r^2\sin^2\sigma) +$$
$$+\sqrt{b^2-1}\cdot\sqrt{r_1}\cdot\left[(a-1-r\cos\sigma)\cdot\sin\frac{\beta'}{2} + r\cdot\sin\sigma\cdot\cos\frac{\beta'}{2}\right]$$

REFERENCES

1. Mockmoore, C.A. (1944), "Flow Around Bends in Stable Channels", Transactions, A.S.C.E., Vol. 109.

2. Shukry, A. (1950), "Flow Around Bends in an Open Flume", Transactions, A.S.C.E., Vol. 115.

3. Rozovskii, I.L. (1957), "Flow of Water in Bends of Open Channels", A.S.U.S.S.R., Translated by the Israel Program for Scientific Translations, 1961.

4. Hayat, S. (1965), The Variation of Loss Coefficient with Froude Number in an Open Channel Bend, M. S. Thesis, Univ. of Iowa, Iowa City.

5. Yen, B. C. (1965), Characteristics of Subcritical Flow in a Meandering Channel, Iowa Institute of Hydraulic Research, Iowa City.

6. Yen, C.L. (1967), Bend Configurations and Characteristics of Subcritical Flow in a Meandering Channel, Ph.D. Thesis, Univ. of Iowa, Iowa City.

7. Bachmeteff, B. C. (1932), Hydraulics of Open Channels, McGraw-Hill Book Co., New York.

8. Chow, V.T. (1959), Open -Channel Hydraulics, McGraw-Hill Book Co., New York.

9. Reinus, E. (1961), "Steady Uniform Flow in Open Channels", Division of Hydraulics, Roy. Inst. of Tech., Stockholm, Bulletin No. 60.

10. Gurevich, M. I. (1965), Theory of Jets in Ideal Fluids, Academic Press, New York.

11. Duisheev, E. (1958), "Studies on the Theory of Spillways", Izv. Vyssh. Uchebn. Zavedenii, Matem.

12. Zhukovskii, N. E. (1949), Collected Works, Vol. 2, Gostekhizdat, Moscow.

13. Lapidus, L. (1962), Digital Computations for Chemical Engineers, McGraw-Hill Book Co, New York.